Suppression of magnetic ordering in quasi-one-dimensional $Fe_xCo_{1-x}Nb_2O_6$ compounds

P. W. C. Sarvezuk,[1,2] E. J. Kinast,[3] C. V. Colin,[2] M. A. Gusmão,[1] J. B. M. da Cunha,[1] and O. Isnard[2,*]

[1]*Instituto de Física, Universidade Federal do Rio Grande do Sul, C.P. 15051, 91501-970 Porto Alegre, Brazil*

[2]*Institut Néel (CNRS) and Université Joseph Fourier, B.P. 166, F-38042 Grenoble Cedex 9, France*

[3]*Universidade Estadual do Rio Grande do Sul, Rua Inconfidentes 395, 93340-140 Novo Hamburgo, Brazil*

(Received 30 December 2010; published 5 May 2011)

We present a systematic investigation of the series of compounds $Fe_xCo_{1-x}Nb_2O_6$ by means of x-ray and neutron powder diffraction combined with magnetic measurements, carried out in the paramagnetic as well as in the ordered state, to probe the stability of the magnetic ordering against the composition changes in this model Ising system. Fe for Co substitution induces a continuous lattice volume increase, preserving the orthorhombic crystal structure. The unit-cell expansion is anisotropic and occurs mainly in the *ab* plane. The observed magnetic structures for $x = 0, 0.8$, and 1 are described by the propagation vectors $(0,1/2,0)$ and $(1/2,1/2,0)$, and are consistent with the picture of ferromagnetic Ising-type chains of Fe/Co spins antiferromagnetically coupled by weak interchain interactions. We find out that for $0 < x < 0.8$, substitution tends to suppress magnetic order, with the studied compounds remaining disordered down to 1.7 K. Our estimate of the exchange integrals for the ordered compound at $x = 0.8$ indicates that the Fe/Co cation disorder induces a substantial drop of the average exchange strength both within and between the Ising chains, reflecting the tendency to suppression of long-range magnetic order.

DOI: 10.1103/PhysRevB.83.174412 PACS number(s): 75.25.−j, 75.30.Cr, 75.47.Lx

I. INTRODUCTION

The MX_2O_6 (M = Mn, Fe, Co, Ni, Cu; X = Ta, Nb) compounds have attracted much interest because of their low-dimensional magnetic characteristics. Whereas the MTa_2O_6 compounds are tetragonal and present quasi-two-dimensional magnetic behavior,[1,2] the crystal structure of MNb_2O_6 belongs to the *Pbcn* orthorhombic space group,[3,4] or colombite structure, which yields quasi-one-dimensional magnetism.[3–5] The structure can be viewed as a stacking of slightly tilted oxygen octahedra surrounding the cations, forming zigzag chains along the *c* axis. Such zigzag chains are also characteristic of the α-PbO_2 structure.[6,7] Two of the three oxygen octahedra contain Nb^{5+}, and one contains M^{2+} ions. As reported earlier,[8] the octahedra surrounding the M^{2+} cations are quite distorted, so that this structure can alternatively be described as resulting from layers of distorted hexagonal-closed-packed octahedra perpendicular to the *a* axis, and following the sequence of cations M-Nb-Nb-M-Nb-Nb-M. Figure 1 depicts a unit cell of the structure, with octahedra surrounding Nb^{5+} and M^{2+} cations drawn in different colors (shades).

The MNb_2O_6 compounds with M = Co and Fe have been the subject of detailed investigations. $CoNb_2O_6$ has been found to order at 2.9 K, with a transition from the paramagnetic phase to an ordered spin structure incommensurate with the lattice.[9] This is followed near 2 K by a second transition to a commensurate antiferromagnetic (AF) order in which the magnetic unit cell is doubled with respect to the crystal cell along the *c* axis.[10] The magnetic phase diagram of $CoNb_2O_6$ was investigated combining powder and single crystal neutron diffraction by Schärf *et al.*,[9] and later by Heid *et al.*[3,4] and Kobayashi *et al.*[5] This system has also been studied by nuclear magnetic resonance (NMR),[11,12] electron-spin resonance (ESR),[11] and infrared-transmission spectroscopy.[12] Recently, quantum-critical behavior consistent with the transverse-field Ising model in one dimension and exotic-symmetry excitations were observed[13] by inelastic neutron scattering on a single crystal of $CoNb_2O_6$. This experimental study was followed by a theoretical investigation of the interplay between quantum criticality and geometric frustration in the same system, still in the presence of a transverse magnetic field.[14]

The magnetism in $FeNb_2O_6$ was first reported by Weitzel *et al.*,[15] and it was later studied by means of powder and single-crystal neutron-diffraction experiments.[3] Whereas a collinear magnetic structure with propagation vector $(0,1/2,0)$ was first reported,[15] a noncollinear canted structure was later deduced from magnetization studies as well as group theoretical considerations.[16,17] More recently, Heid and coworkers[3] have established the presence of two propagation vectors, $(0,1/2,0)$ and $(1/2,1/2,0)$, on the basis of magnetic measurements combined with neutron diffraction carried out on both powder and single crystals.

We recently reinvestigated the magnetic phase diagram of $CoNb_2O_6$ by means of a combined analysis of powder neutron-diffraction and magnetization measurements.[18] We now focus our attention on the $Fe_xCo_{1-x}Nb_2O_6$ isotype compounds, which exhibit the same crystal structure including the presence of weakly coupled Ising chains. In this paper, we report on the evolution of structural and magnetic properties with the transition-metal composition along the $Fe_xCo_{1-x}Nb_2O_6$ series. We find a smooth evolution of lattice parameters as well as effective magnetic moments in the paramagnetic phase. However, positional disorder of the magnetic cations turns out to be very relevant, and extremely deleterious to the magnetic ordering. Even though $FeNb_2O_6$ and $CoNb_2O_6$ present stable magnetic phases at low temperature, such an order is suppressed for most of the compounds in the series, at least above the lowest temperature (1.7 K) investigated.

The paper is organized as follows. Section II is devoted to a description of the experimental techniques employed. Our main results are presented and discussed in Sec. III, covering structural properties obtained from x-ray diffraction (Sec. III A), structural and magnetic investigations through

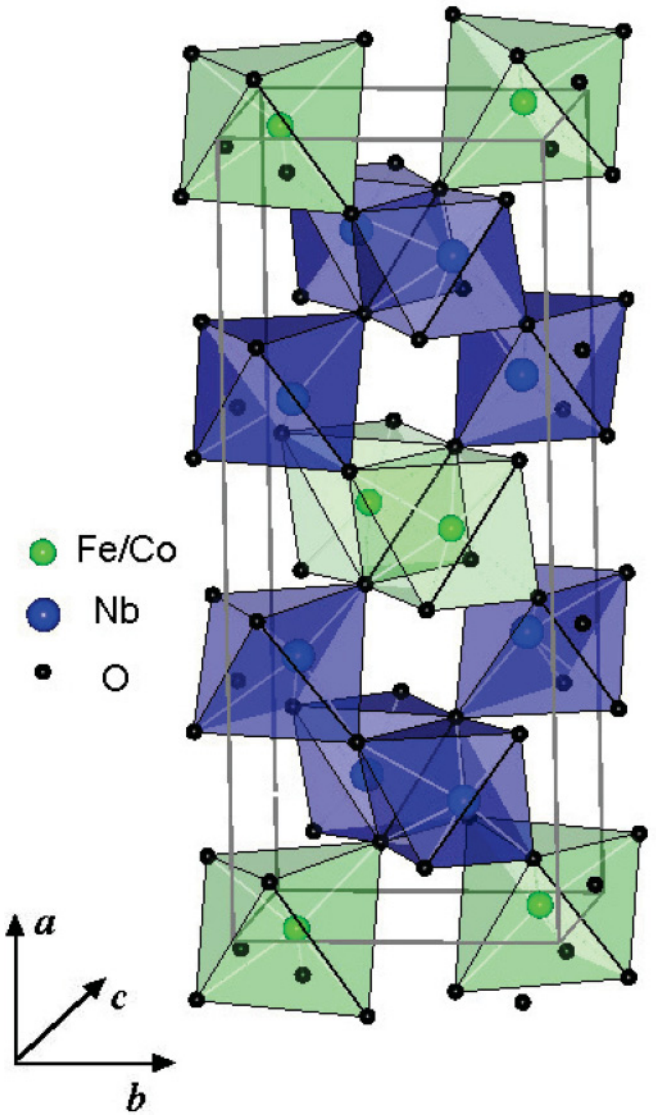

FIG. 1. (Color online) Crystal structure of the $Fe_xCo_{1-x}Nb_2O_6$ series of compounds, showing the oxygen octahedra surrounding the Fe/Co and Nb ions.

neutron-diffraction experiments (Sec. III B), measurements of magnetic susceptibility and magnetization (Sec. III C), and finishing with an evaluation of exchange couplings from the susceptibility data (Sec. III D). Concluding remarks are presented in Sec. IV.

II. EXPERIMENTAL DETAILS

Powder samples were prepared with appropriate amounts of Fe_2O_3, powder metallic Fe and Nb_2O_5 for $FeNb_2O_6$, and Co_3O_4 and Nb_2O_5 for $CoNb_2O_6$. The mixtures were ground, pressed into pellets, and heat-treated in vacuum for $FeNb_2O_6$ and in air for $CoNb_2O_6$ at 1370 K for 24 and 30 h, respectively. To obtain powder $Fe_xCo_{1-x}Nb_2O_6$, stoichiometric amounts of $FeNb_2O_6$ and $CoNb_2O_6$ were mixed, regrinded, and heat-treated for 24 h in vacuum at 1370 K. The obtained samples were slowly cooled and powdered down to a maximum grain size of about 40 μm. The samples were found to be stable in air at ambient conditions, with x-ray patterns reproduced after several months. A large amount of sample, of about 2.5 g, was prepared for the neutron-diffraction (ND) measurements.

Sample purity was first checked by x-ray diffraction (XRD) analysis before undertaking magnetic or neutron measurements. The XRD was performed in Bragg-Brentano geometry, using Co $K\alpha$ radiation, $\lambda(K\alpha_1)$ = 1.7890 Å and $\lambda(K\alpha_2)$ = 1.7928 Å, with a scan step of 0.05° and angular 2θ range from 10° to 80°.

Magnetic measurements were undertaken on powder samples in a wide temperature range, from 1.7 to 300 K, using an extraction magnetometer or a SQUID. Isothermal magnetization curves were recorded in magnetic fields ranging from $\mu_0 H = 0$ to 10 T, and the magnetic susceptibility as a function of temperature was measured at 0.5 T (extraction) or 5.0 mT (SQUID). For better accuracy, magnetic susceptibility values above 50 K have been confirmed by extrapolating the magnetization data down to zero applied field via *Arrott plots* of the isothermal magnetization.[19]

In the powder ND measurements, data collection was done with the double-axis multicounter high-flux diffractometer D1B operated by the CNRS at the Institut Laue Langevin (ILL), Grenoble, using a 2.52-Å wavelength selected by a pyrolytic graphite monochromator. D1B is a powder diffractometer operating with the takeoff angle of the monochromator at 44° (in 2θ). In the configuration used, the resolution was about 0.3° (full width at half maximum), and the multicounter was composed of 400 cells covering a total angular domain of 80° (in 2θ). The used angular 2θ range was from 5° to 85° with a detector step of 0.2°.

Analysis of XRD and ND data was done using the FULLPROF refinement package[20] to extract the crystallographic and magnetic parameters. Agreement factors used in this paper are defined according to the guidelines of the Rietveld refinement, which can be found elsewhere.[21] The neutron scattering lengths used were 0.7054×10^{-12} cm for Nb, 0.9450×10^{-12} cm for Fe, 0.2490×10^{-12} cm for Co, and 0.5803×10^{-12} cm for O; values were taken from Sears.[22]

III. RESULTS AND DISCUSSION

A. X-ray diffraction

According to our analysis of the XRD patterns, all the (Fe,Co)Nb_2O_6 samples present a single phase, and the *Pbcn* space-group symmetry is preserved. As an example, the Rietveld analysis of the XRD pattern recorded at room temperature for $Fe_{0.4}Co_{0.6}Nb_2O_6$ is shown in Fig. 2. Lattice and position parameters derived from the Rietveld refinement at room temperature are listed in Table I together with the agreement factors of the refinements.

Figure 3 presents the composition dependence of the unit-cell volume at both 300 and 20 K (the last one obtained from ND). In general, Fe for Co substitution was found to induce an essentially linear increase of the unit-cell volume, with approximately the same rate at both temperatures. The unit cell evolves anisotropically: the lattice parameter a is very sensitive to Fe content, increasing continuously with x; b also increases, while c is much less affected by composition, and can be considered as constant within the experimental error bars.

TABLE I. Crystal structure data and agreement factors as obtained from Rietveld refinement of the room-temperature x-ray diffraction pattern for the indicated compositions (first line) in the $Fe_xCo_{1-x}Nb_2O_6$ series of compounds.

$x \rightarrow$		0.0	0.2	0.4	0.6	0.8	1.0
	x	0	0	0	0	0	0
Fe/Co	y	0.1599(14)	0.157(4)	0.163(4)	0.153(4)	0.144(3)	0.1683(16)
	z	0.25	0.25	0.25	0.25	0.25	0.25
	x	0.1604(20)	0.1601(5)	0.1602(5)	0.1602(5)	0.1604(6)	0.1612(20)
Nb	y	0.3179(5)	0.3176(11)	0.3173(12)	0.3166(12)	0.3153(11)	0.3185(5)
	z	0.7510(17)	0.759(3)	0.755(3)	0.755(4)	0.794(3)	0.7521(14)
	x	0.0968(14)	0.101(3)	0.114(3)	0.107(3)	0.120(3)	0.1082(12)
O1	y	0.396(4)	0.401(9)	0.407(8)	0.413(9)	0.395(9)	0.405(4)
	z	0.436(6)	0.437(12)	0.421(11)	0.427(13)	0.392(10)	0.436(5)
	x	0.0813(13)	0.086(3)	0.089(2)	0.087(3)	0.097(3)	0.0797(12)
O2	y	0.133(4)	0.139(9)	0.130(9)	0.135(9)	0.142(8)	0.115(4)
	z	0.896(5)	0.899(11)	0.908(11)	0.923(13)	0.918(11)	0.910(6)
	x	0.2565(19)	0.256(6)	0.263(4)	0.257(5)	0.270(4)	0.2645(16)
O3	y	0.119(3)	0.117(9)	0.122(9)	0.120(8)	0.106(7)	0.120(4)
	z	0.577(5)	0.582(12)	0.585(11)	0.578(13)	0.577(13)	0.581(5)
a (Å)		14.1307(4)	14.1624(6)	14.1837(8)	14.2077(7)	14.2399(6)	14.2583(7)
b (Å)		5.7015(2)	5.7103(3)	5.7149(3)	5.7197(3)	5.7279(2)	5.7308(2)
c (Å)		5.0370(1)	5.0414(2)	5.0418(2)	5.0431(2)	5.0469(2)	5.0465(2)
R_{wp} (%)		13.7	10.1	11.5	12.2	14	19
R_B (%)		4.7	8.1	8.3	10	11.2	11.4

This indicates that the value of c is mainly determined by the NbO_6 octahedra rather than by the $(Fe,Co)O_6$ ones. From XRD refinements, we calculated the edge-length distortion (ELD)[23] of the octahedra, i.e., the root-mean-square deviation of the edge lengths. Both $(Fe,Co)O_6$ and NbO_6 octahedra are found to present positive ELD values, but octahedra surrounding the Fe or Co cations are less distorted than the Nb ones. The ELD values range from about 4% to 12%, growing with Fe content.

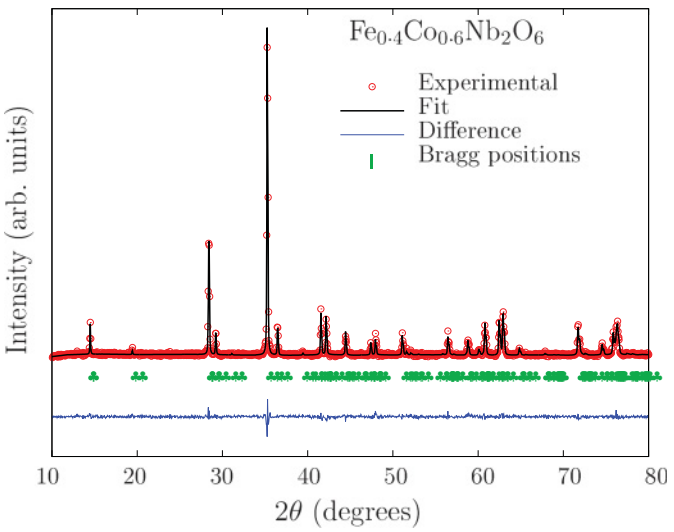

FIG. 2. (Color online) Rietveld refinement of the x-ray diffraction pattern ($\lambda = 1.790$ Å) recorded at room temperature for $Fe_{0.4}Co_{0.6}Nb_2O_6$. The Bragg positions correspond to the *Pbcn* space group. The Rietveld refinement agreement factors are $R_{wp} = 11.5\%$ and $R_B = 8.3\%$.

The structural data in Table I allow us to observe changes in the distortion of the magnetic ion environment with composition. In the Co-rich side of the series, four Fe/Co-O distances are almost equal, near 2.14 Å, while the two others are about 2.10 Å, and correspond to apically opposite oxygens. This means that the deformation of the oxygen octahedron surrounding a magnetic cation is close to a compression along one of the principal axes. In contrast, the Fe-rich side exhibits three sets of Fe/Co-O distances, typically 2.07, 2.13, and 2.25 Å, and only the first one occurs for a pair of apically opposite anions. Thus, the octahedron deformation breaks the nearly axial symmetry observed in the previous case. This

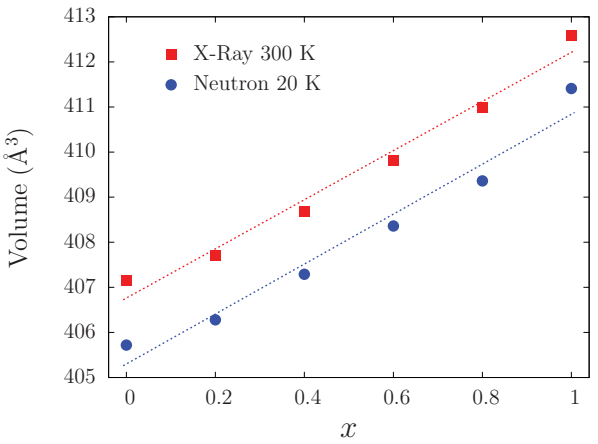

FIG. 3. (Color online) Concentration dependence of the unit-cell volume of the $Fe_xCo_{1-x}Nb_2O_6$ compounds. Squares and circles correspond to x-ray at room temperature and neutron diffraction at 20 K, respectively. The values for $CoNb_2O_6$ are from Ref. 4.

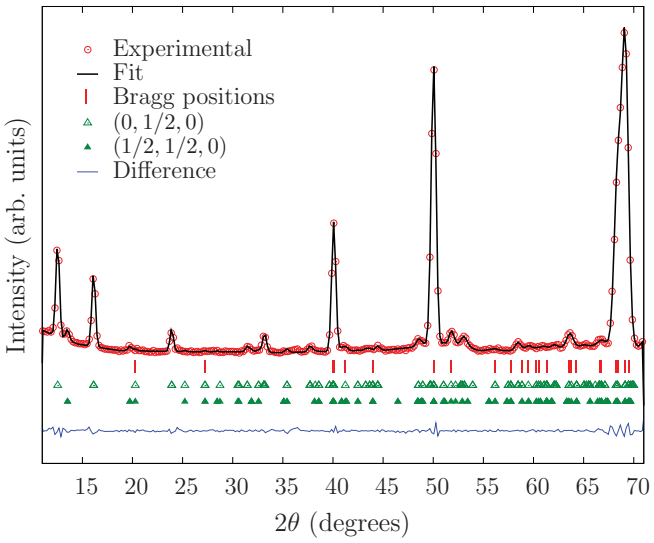

FIG. 4. (Color online) Refinement of the neutron powder diffraction pattern ($\lambda = 2.52$ Å) recorded at 1.7 K for the $Fe_{0.8}Co_{0.2}Nb_2O_6$ compound. Triangles indicate magnetic reflections, and it can be seen that the structure with propagation vector $(0,1/2,0)$ is dominant. The Rietveld refinement agreement factors are $R_{wp} = 1.8\%$, $R_B = 1.6\%$, and $R_{mag} = 15.3\%$ and 30.2% for $(0,1/2,0)$ and $(1/2,1/2,0)$ propagation vectors, respectively.

is relevant to the analysis of magnetic moment orientations determined from ND.

B. Neutron diffraction

To investigate the magnetic structure, low-temperature neutron-diffraction patterns have been recorded at 1.7 and 20 K. As can be seen from the fitted ND pattern of $Fe_{0.8}Co_{0.2}Nb_2O_6$ shown in Fig. 4, the crystal structure is preserved at low temperature. The positions of the oxygen atoms have been confirmed by ND, which is known to be more sensitive to the position of light elements than XRD. This iron-rich compound is well ordered at 1.7 K, leading to sharp magnetic Bragg reflections observed in Fig. 4. The neutron-diffraction pattern analysis of this compound shows that the magnetic structure is similar to that reported for $FeNb_2O_6$.[24] The magnetic peaks can be indexed using two propagation vectors: $(1/2,1/2,0)$ and $(0,1/2,0)$, with dominance of the latter, whose structure is schematically shown in Fig. 5. We found 91% of the $(0,1/2,0)$ phase and 9% of the $(1/2,1/2,0)$ phase for the $FeNb_2O_6$ compound. Following the interpretation of single-crystal analysis reported previously,[4] one can expect the presence of domains with two different magnetic structures, corresponding to each of the propagation vectors. In our refinement, the magnetic moment has been constrained to be the same at all magnetic sites for both propagation vectors. The results of ND refinement for $Fe_{0.8}Co_{0.2}Nb_2O_6$ at 1.7 K are summarized in Table II. For the atomic positions shown in that table, the first two quoted magnetic moments belong to one chain, and the other two to a different one. The whole magnetic structure (partially depicted in Fig. 5) is then obtained from those four moments and the propagation vector.

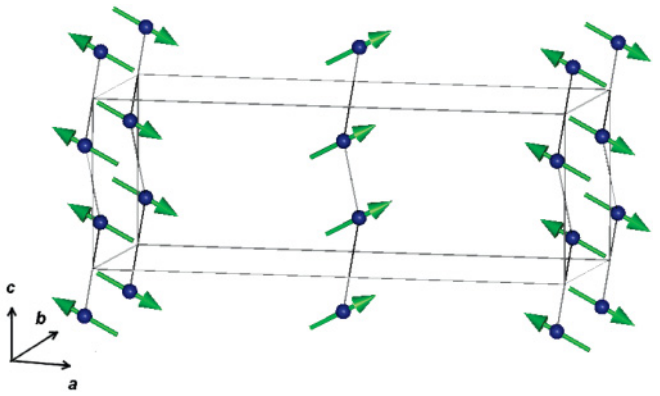

FIG. 5. (Color online) Schematic drawings of the magnetic structure with propagation vector $(0,1/2,0)$, which is the major phase present in the ordered compounds of the $Fe_xCo_{1-x}Nb_2O_6$ series.

For $FeNb_2O_6$, the magnetic moments were found[4] to be tilted away from the c axis along the zigzag chains, with a canting angle of about 23°–24°. Similar behavior is found here, but with a slightly larger angle. A magnetic moment of 3.2 μ_B is refined for $Fe_{0.8}Co_{0.2}Nb_2O_6$, with a tilt angle of 28° at 1.7 K. This is intermediate between the above value for $FeNb_2O_6$ and the one for $CoNb_2O_6$, which is near 31°, essentially aligned with the shortened principal axis of the oxygen octahedron that we mentioned in Sec. III A. This coincidence is due to the axial symmetry of the deformed octahedron, which no longer exists upon Fe substitution. Thus, in the latter case the magnetic easy axis arising from crystal-field anisotropy does not coincide with one of the principal axes of the distorted octahedron. The average Fe/Co magnetic moment is smaller than the value reported[17] for $FeNb_2O_6$. We attribute this difference to the proximity of the ordering temperature, which is only 2.4 K for $Fe_{0.8}Co_{0.2}Nb_2O_6$ against 4.9 K for $FeNb_2O_6$. In addition, given that there are two coexisting magnetic phases, it is possible that part of the sample is not ordered at all, leading to an underestimation of magnetic moments from diffraction-peak intensities.

In contrast to what we observed for the iron-rich compound with $x = 0.8$, the samples with lower Fe concentrations do not reproduce the same magnetic behavior. The ND pattern

TABLE II. Magnetic-refinement results of neutron-diffraction data obtained at 1.7 K for $Fe_{0.8}Co_{0.2}Nb_2O_6$. The quoted magnetic moments correspond to the phase with propagation vector $(0,1/2,0)$. All atomic positions refer to the same vertex of a given crystallographic unit cell

Fe/Co position[a]	Magnetic moment (μ_B)
$(0,\ y,\ \frac{1}{4})$	$(-1.5, 0.0, 2.8)$
$(0,\ -y,\ \frac{3}{4})$	$(-1.5, 0.0, 2.8)$
$(\frac{1}{2},\ \frac{1}{2}+y,\ \frac{1}{4})$	$(1.5, 0.0, 2.8)$
$(\frac{1}{2},\ \frac{1}{2}-y,\ \frac{3}{4})$	$(1.5, 0.0, 2.8)$
Propagation vector	Volume fraction
$(0,1/2,0)$	85%
$(1/2,1/2,0)$	15%

[a] $y \simeq 0.16$ in units of the corresponding lattice parameter.

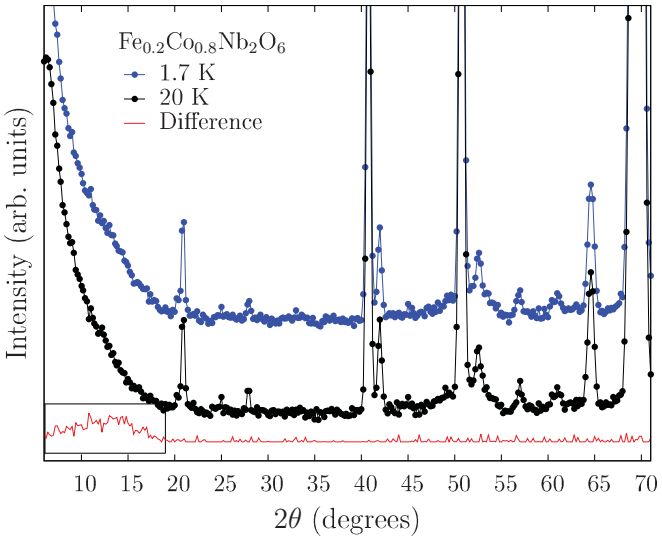

FIG. 6. (Color online) Comparison of the neutron-diffraction patterns recorded at 1.7 and 20 K for $Fe_{0.2}Co_{0.8}Nb_2O_6$. A difference plot is shown at the bottom, with a rectangle on the left highlighting an indication of magnetic diffuse scattering.

for $Fe_{0.2}Co_{0.8}Nb_2O_6$ is plotted in Fig. 6. Refinement of the diffraction pattern demonstrates that the crystal structure remains the same (which is true for all the investigated compounds), but the spectrum does not exhibit extra reflections originating from magnetic order.

A difference pattern was calculated by subtracting the pattern recorded at 20 K from that recorded at 1.7 K. As can be seen in Fig. 6, this difference pattern exhibits a broad signal around $2\theta = 11.5^\circ$, but no magnetic Bragg reflections, confirming that the sample is not magnetically ordered. Similar results have been obtained for $x = 0.4$ and 0.6. The presence of such a broad signal of magnetic origin at 1.7 K, which is indicative of short-range order, may imply that the system is approaching a magnetically ordered state at a still lower temperature, but could also be due to short-range correlations in a disordered state due to suppression of long-range order by frustration. To distinguish between these two hypotheses, further neutron-diffraction studies at very low temperature are necessary. The maximum of the short-range diffuse magnetic scattering is observed at a wave vector $q_m \simeq 0.5$ Å^{-1}. Similar values are found for the $x = 0.4$, 0.6, and 0.8 compounds. It is noticeable that this position in reciprocal space is close to where the two most intense magnetic Bragg peaks of the (0,1/2,0) structure appear in the ordered compounds. To obtain information about the short-range correlations yielding the diffuse scattering signal, we have used a model first proposed by Bertaut and Burlet[25] for spin glasses, and later utilized by Greedan *et al.*[26] for pyrochlores. In this model, the cross section for magnetic scattering due to short-range order is expressed as a sum of radial functions $\sin(qR_i)/qR_i$ with coefficients proportional to the correlations between spins at relative distances R_i in the lattice. Even though the weakness of the observed magnetic signal does not allow us to follow many oscillations, we were able to reach semiquantitative conclusions: (i) the correlation length is not much larger than the distance between nearest chains along the [110] direction, which is about 7.6 Å; (ii) the intrachain spin-spin correlations are ferromagnetic while the interchain ones are dominantly AF, both of comparable net magnitude in the sum.

At this point it is worthwhile to stress that the crystal structure of the studied compounds is not significantly modified upon Fe for Co substitution except for expansion of the unit cell, and some distortion of the oxygen octahedra. Consequently, the destruction of magnetic order cannot be attributed to large modifications of crystal structure occurring upon substitution. This change of magnetic properties probably results from the induced cationic disorder as well as the possible occurrence of competing exchange interactions. Indeed, the existence of competing antiferromagnetic interactions within a nearly triangular net of ferromagnetic chains in the MNb_2O_6 structure has been extensively discussed.[5,14,27] The tendency to magnetic frustration of such a structure seems to be enhanced by substitutions like those discussed here.

C. Magnetic measurements

Sufficiently above the ordering temperature, measured values of the paramagnetic susceptibility as a function of temperature were fitted to the Curie-Weiss law, $\chi(T) = C/(T - \theta_W)$. As can be seen in Fig. 7, the magnetic susceptibility exhibits a typical Curie-Weiss behavior at high temperature for the Fe-rich samples. However, data for Co-rich samples were corrected for a positive, temperature-independent χ_0, but still show some anomalous temperature behavior, departing from the Curie-Weiss law at high temperatures. This can be interpreted as a Van Vleck paramagnetic contribution of the Co^{2+} cations, which can present a small separation between the two lowest energy multiplets, depending on the local crystal field.[28,29] At moderate temperatures, the usual Van Vleck mechanism yields the constant χ_0 contribution, while population of the upper level at higher temperatures gives rise to the additional temperature-dependent contribution. Indeed, we noticed that these effects are less pronounced in measurements performed with an extraction magnetometer, where typically the measuring field corresponds to $\mu_0 H = 0.5$ T, and more noticeable when using a SQUID, with $\mu_0 H = 5.0$ mT. This is consistent with a Zeeman enhancement of the splitting between the two levels involved in this effect, since they correspond to different total spin.

The Weiss temperature θ_W, Curie constant C, and effective magnetic moments μ_{eff} obtained for the various samples are listed in Table III. As can be seen, the effective magnetic moment varies between 4.40 and 5.42 μ_B from $x = 0$ to 1. These limiting values are in excellent agreement with observations[30,31] for Co^{2+} and Fe^{2+}, and within the usual ranges for these cations in an octahedral environment. The values of θ_W are rather small, and are all positive, despite the fact that both $CoTa_2O_6$ and $FeNb_2O_6$ order antiferromagnetically at very low temperatures. This is actually expected, since the MNb_2O_6 compounds are known to exhibit ferromagnetic intrachain interactions along the c axis, and much weaker antiferromagnetic interchain couplings.[5,24] Thus, the high-temperature behavior is dominated by the ferromagnetic intrachain interactions, while AF ordering ultimately sets in due to the interchain coupling.

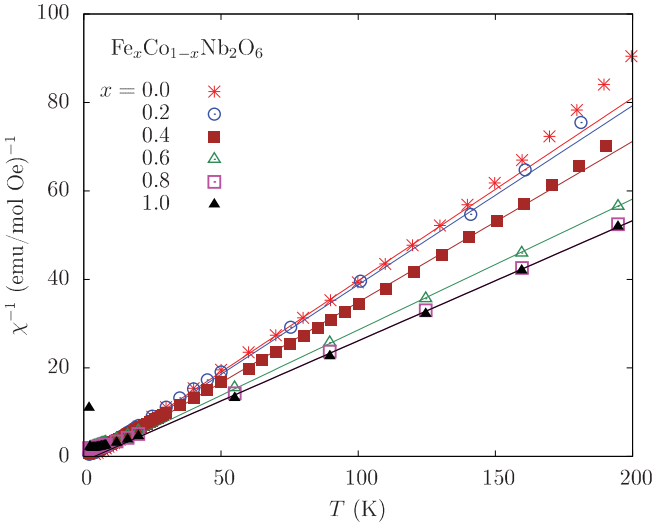

FIG. 7. (Color online) Fitting of the inverse susceptibility to the Curie-Weiss law for all the studied samples, after subtraction of a constant Van Vleck contribution. Notice the departure from the straight line at high temperatures for samples with high Co concentration, as discussed in the text.

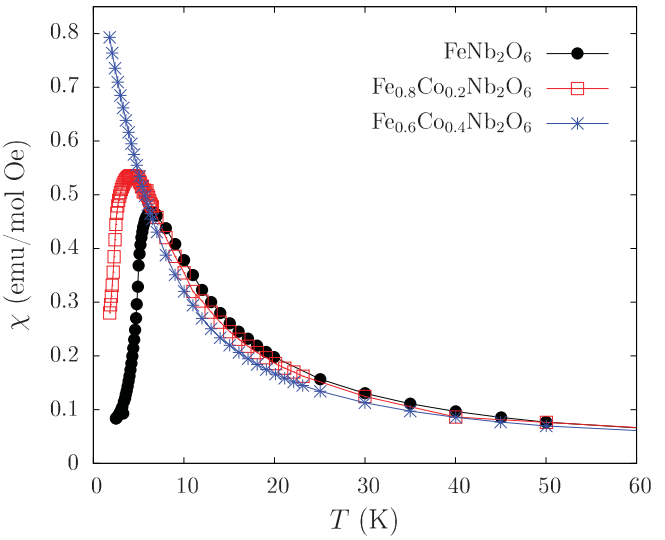

FIG. 8. (Color online) Low-temperature dependence of the dc susceptibility recorded at $\mu_0 H = 0.05$ T for $FeNb_2O_6$, $Fe_{0.8}Co_{0.2}Nb_2O_6$, and $Fe_{0.6}Co_{0.4}Nb_2O_6$. Notice that there is no indication of ordering for the latter down to temperatures slightly below 2 K.

At intermediate compositions in the series, the situation is more complex. Figure 8 shows the thermal variation of the magnetic susceptibility obtained for $FeNb_2O_6$, and for the samples with Fe concentrations of 0.8 and 0.6, for comparison. Unlike the compounds with $x = 1.0$ and 0.8, which present a drop of the susceptibility at low temperature, the $x = 0.6$ compound does not show any sign of a magnetic transition. The same qualitative behavior is observed for the $x = 0.4$ and 0.2 samples. This is in agreement with our findings from ND, as discussed in Sec. III B.

A typical magnetization curve recorded for $FeNb_2O_6$ at 3 K is plotted in Fig. 9. A metamagnetic transition is observed at a field corresponding to $\mu_0 H = 0.95(\pm 0.03)$ T, a result in excellent agreement with the data reported earlier by Heid *et al.*[4] Such a transition can be easily interpreted as resulting from spin flipping the ferromagnetic chains, which are kept in an overall AF structure by very weak interchain interactions. It is worth noticing that there is no hysteresis in the magnetization curves, except for a small one in the spin-flipped (high-field) part, which should be due to pinning of the chains. The highest magnetic moment in Fig. 9 is close to 3.2 μ_B/f.u., at $\mu_0 H =$ 10 T. This value is substantially lower than the effective moment obtained from the paramagnetic susceptibility (Table III), but we must keep in mind that it is difficult to reach saturation due to the random orientations between chain axes and magnetic field in powder samples. As can be seen in Fig. 9, the spin-flip transition can still be observed for $x = 0.8$ as a change of slope near $\mu_0 H \simeq 0.92(\pm 0.03)$ T, but it is clearly smoothed out. We also observe a decrease of the high-field magnetization value for this composition. However, these differences are not exclusively due to Co for Fe substitution, but probably also a consequence of the proximity of the Néel temperature, as already pointed out above.

Moving now to the opposite end of the series, the isothermal magnetization curves of $Fe_{0.2}Co_{0.8}Nb_2O_6$ are gathered in

TABLE III. Parameters characterizing the paramagnetic state of the $Fe_xCo_{1-x}Nb_2O_6$ compounds as obtained from measurements of dc susceptibility.

x	θ_W (K)	C (emu K/mol Oe)	μ_{eff} (μ_B)
0	3.9 (±1.3)	2.42	4.40
0.2	4.2 (±1.5)	2.47	4.44
0.4	4.2 (±1.5)	2.75	4.69
0.6	3.4 (±1.5)	3.38	5.17
0.8	3.3 (±1.4)	3.65	5.40
1	6.6 (±1.1)	3.67	5.42

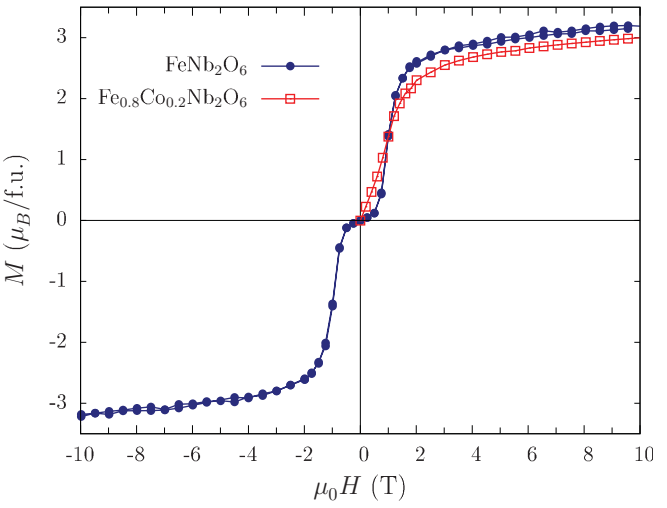

FIG. 9. (Color online) Isothermal magnetization curve recorded at 2 K on powder sample of $Fe_{0.8}Co_{0.2}Nb_2O_6$ compared to the hysteresis cycle recorded for $FeNb_2O_6$ at 3 K, for which a metamagnetic transition is clearly seen.

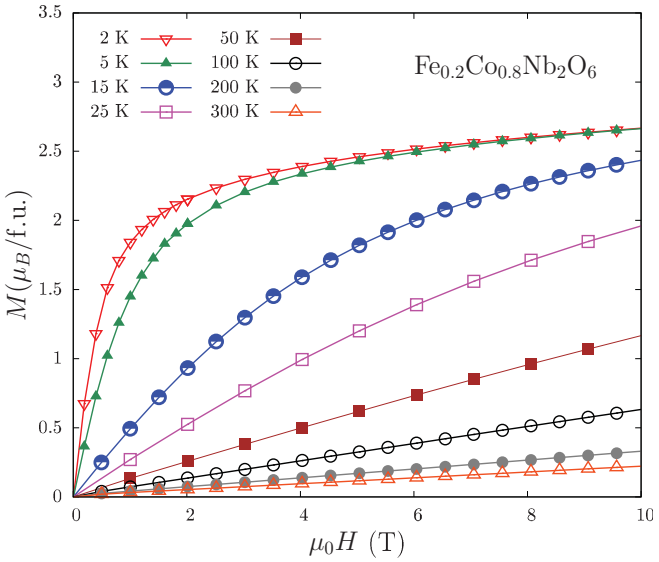

FIG. 10. (Color online) Isothermal magnetization curves recorded at the indicated temperatures for the $Fe_{0.2}Co_{0.8}Nb_2O_6$ compound.

Fig. 10. Since no magnetic order was observed by neutron diffraction down to 1.7 K in this compound, its magnetic behavior above that temperature has to be regarded as a field-induced effect. The isothermal curves show an overall ferromagnetic behavior at the lowest temperatures appearing in Fig. 10. This may be interpreted as a stabilization of ferromagnetic ordering of the spin chains by the applied field. Indeed, as nicely discussed in Ref. 13, a magnetic field applied parallel to the Ising spins induces a gap to the kink excitations that otherwise would suppress ferromagnetic order at finite temperature for free chains.

D. Exchange constants

Within the scenario of weakly interacting Ising chains, we can actually predict values of the exchange constants from our susceptibility data and Néel temperatures. The exact partition function of an isolated Ising chain in the presence of an applied magnetic field (along the spin axis) is well known.[32] Taking into account that our "Ising" spins have module S, but leaving out factors of $g\mu_B$, the resulting expression for the magnetization as a function of field and temperature is

$$M(H,T) = S\frac{e^{2S^2J_0/T}\sinh(SH/T)}{[e^{4S^2J_0/T}\sinh^2(SH/T)+1]^{1/2}}. \quad (1)$$

We can now treat the interchain interaction at the mean-field level, replacing the external field in Eq. (1) by an effective field given by

$$H^{\text{eff}} = H + z_\perp J_\perp M. \quad (2)$$

Here, we are considering that $J_\perp$ is an average exchange between a spin in a given chain and its neighbors on the bc plane in all the six closest chains ($z_\perp = 6$). Actually, since this plane is not strictly an equilateral triangular lattice but rather formed by isosceles triangles, there are two neighbors interacting with an exchange J_1 and the other four with a different one, J_2, but of similar intensities.[14]

Keeping only terms of first order in M or H in Eq. (1), we obtain the paramagnetic susceptibility as

$$\chi = \frac{1}{\chi_0^{-1} - z_\perp J_\perp}, \quad (3)$$

where

$$\chi_0 = \frac{S^2}{T}e^{2S^2J_0/T} \quad (4)$$

is the isolated-chain susceptibility. At high temperatures, expanding the exponential up to linear order in $1/T$, Eq. (3) assumes the usual Curie-Weiss form, $\chi = C/(T-\theta_W)$, with

$$\theta_W = (2J_0 + z_\perp J_\perp)S^2. \quad (5)$$

On the other hand, if we consider the ordered phase at zero external field, equating the linear coefficients of M on both sides of Eq. (1) yields an expression to determine T_N or, conversely, the interchain exchange interaction,

$$z_\perp^* |J_\perp| S^2 = T_N e^{-2S^2J_0/T_N}. \quad (6)$$

Now, we take $z_\perp^* = 2$ because four of the six interchain interactions tend to cancel each other in the observed ordered phases[18] (see Sec. III B), as discussed earlier[3] for the Fe and Ni compounds.

Knowing T_N and θ_W from the experimental results allows the determination of J_0 and $J_\perp$ through Eqs. (5) and (6). For $CoNb_2O_6$, using the highest transition temperature $T_N = 2.9$ K (even though the ensuing AF order is incommensurate), we obtain $J_0^{\text{Co}} \simeq 1.18$ K (in units of k_B) and $J_\perp^{\text{Co}} \simeq -0.104$ K. The corresponding results for $FeNb_2O_6$, for which[3] $T_N = 4.9$ K, are $J_0^{\text{Fe}} \simeq 1.12$ K and $J_\perp^{\text{Fe}} \simeq -0.098$ K. Our results for the Co compound are in reasonable agreement with those reported by Kobayashi *et al.*,[5] observing that their value of J_0 is probably underestimated because they use a mean-field approach for all interactions, while we start with the exact solution for the chains.

Unfortunately, we cannot study in more detail how the exchange couplings vary with x in the $Fe_xCo_{1-x}Nb_2O_6$ series since the suppression of magnetic order prevents the knowledge of T_N values, despite the fact that Weiss temperatures are determined (see Table III). Actually, the compound with $x = 0.8$ does present an ordered phase below 2.4 K. If we apply the above procedure, with a simple virtual-crystal approximation for the spin, we obtain $J_0 \simeq 0.61$ K and $J_\perp \simeq -0.052$ K. We believe that such a substantial reduction of the effective exchange constants is an artifact of the approximation. It probably indicates that mean-field variations due to cation disorder are very important, and tend to reduce the stability of an ordered state. One has to bear in mind that cation disorder has two main effects: (i) the occurrence of different magnetic moments in the cation environment, thus leading to changes in the local effective magnetic field; (ii) a steric effect of different cation sizes that induce local structural distortion, with consequent modification of exchange integrals. To better understand this point, one has to look at the ab-plane projection of the dominant magnetic structure, with propagation vector $(0,1/2,0)$, as shown in Ref. [3]. In the pure case, selecting a given chain, the net effective field from its six neighboring chains is due to only two of them, along the b direction,

with the contributions from the other four canceling out in the sum. Magnetic cation substitutions on these neighboring chains break this cancellation, allowing for new competing interactions that can enhance frustration and reduce the net effective field. This interchain frustration is probably the most important effect in suppressing magnetic order. The intrachain ferromagnetic interaction should not be significantly affected by cation disorder, but we have to bear in mind that this interaction alone does not yield long-range order at any finite temperature.

IV. CONCLUSIONS

To summarize, our x-ray and neutron-diffraction study of the $Fe_xCo_{1-x}Nb_2O_6$ series of compounds shows that Fe for Co substitution in $CoNb_2O_6$ preserves the orthorhombic crystal structure, and induces a continuous increase of the lattice volume. The expansion occurs mainly along the *a* and *b* axes. Also worth mentioning is the reduction of local symmetry at the magnetic sites due to nontrivial distortion of the surrounding oxygen octahedra. Investigation of the magnetic properties shows that all the compounds exhibit small Néel and Weiss temperatures, consistent with the quasi-one-dimensional nature of their magnetic subsystem. Our ND results and magnetic measurements show that magnetic order is preserved in the Fe-rich region ($x = 0.8$), while no order is established down to 1.7 K for $x = 0.2$, 0.4, and 0.6, in spite of the observation of short-range magnetic correlations. This is in contrast to the quasi-two-dimensional (Fe,Co)Ta_2O_6 systems,[33,34] where Fe for Co substitution was found to preserve the magnetic order. The lower strength of magnetism in (Fe,Co)Nb_2O_6 compounds can be traced to their different crystal structure, in particular the existence of weakly interacting magnetic chains, as well as topological frustration due to the triangular arrangement of these chains with respect to the transverse *ab* plane of the lattice.

In this context, it is clear that an important ingredient is the quasi-one-dimensional magnetic character of these compounds, since a strictly one-dimensional Ising chain is not ordered at finite temperatures. Nevertheless, we should bear in mind that the pure compounds at the two ends of the series are magnetically ordered at low temperatures. The disappearance of this magnetic order for most of the intermediate compounds may result from cation disorder, and consequent changes of the competing interactions that tend to frustrate the ordered state. Indeed, we have shown that a large reduction of the average exchange integrals occurs for $Fe_{0.8}Co_{0.2}Nb_2O_6$, which may also be interpreted as an effect of Fe/Co cation disorder. Further investigation, focused on local changes in the environment of each kind of magnetic ion upon variations of composition, are needed to gain insight into the nature of the disorder effects conjectured here. Experimental studies on (Fe,Co)Nb_2O_6 would also be very useful to probe the complex phase diagram for varying temperature and magnetic field recently predicted[14] in archetypal $CoNb_2O_6$.

ACKNOWLEDGMENTS

This work was supported in part by the French-Brazilian CAPES-COFECUB cooperation program No. 600/08. The Brazilian agency CNPq is also warmly acknowledged. O.I., on behalf of the University Joseph Fourier, is thankful to the Region Rhône Alpes, France, for invaluable support through the ARCUS-Brésil program. The authors also acknowledge interesting discussions with S. R. de Oliveira Neto and C. A. dos Santos at the early stages of this work.

*olivier.isnard@grenoble.cnrs.fr

[1] S. M. Eicher, J. E. Greedan, and K. J. Lushington, J. Solid State Chem. **62**, 220 (1986).
[2] L. I. Zawislak, G. L. F. Fraga, J. B. M. da Cunha, D. Schimitt, A. S. Carriço, and C. A. dos Santos, J. Phys. Condens. Matter **9**, 2295 (1997).
[3] C. Heid, H. Weitzel, F. Bourdarot, R. Calemczuk, T. Vogt, and H. Fuess, J. Phys. Condens. Matter **8**, 10609 (1996).
[4] C. Heid, H. Weitzel, P. Burlet, M. Bonnet, W. Gonschorek, T. Vogt, J. Norwig, and H. Fuess, J. Magn. Magn. Mater. **151**, 123 (1995).
[5] S. Kobayashi, S. Mitsuda, and K. Prokes, Phys. Rev. B **63**, 024415 (2000).
[6] R. W. G. Wyckoff, *Crystal Structure* (Wiley, New York, 1965).
[7] A. I. Zaslavsky, Y. D. Kondrashev, and S. S. Tolkachev, Dokl. Akad. Nauk SSSR **75**, 559 (1950).
[8] P. Bordet, A. McHale, A. Santoro, and R. S. Roth, J. Solid State Chem. **64**, 30 (1986).
[9] W. Scharf, H. Weitzel, I. Yaeger, I. Maartense, and B. M. Wanklyn, J. Magn. Magn. Mater. **13**, 121 (1979).
[10] H. Weitzel and S. Klein, Solid State Commun. **12**, 113 (1973).
[11] T. Kunimoto, K. Nagasaka, H. Nojiri, S. Luther, M. Motokawa, H. Ohta, T. Goto, S. Okubo, and K. Kohn, J. Phys. Soc. Jpn. **68**, 1703 (1999).
[12] T. Kunimoto, M. Sato, K. Nagasaka, and K. Kohn, J. Phys. Soc. Jpn. **68**, 1404 (1999).
[13] R. Coldea, D. A. Tennant, E. M. Wheeler, E. Wawrzynska, D. Prabhakaran, M. Telling, K. Habicht, P. Smeibidl, and K. Kiefer, Science **327**, 177 (2010).
[14] S. Lee, R. K. Kaul, and L. Balents, Nat. Phys. **6**, 702 (2010).
[15] H. Weitzel, Anorg. Allg. Chem. **380**, 119 (1971).
[16] I. Yaeger, A. H. Morrish, and B. M. Wanklyn, Phys. Rev. B **15**, 1465 (1977).
[17] I. Yaeger, A. H. Morrish, B. M. Wanklyn, and B. J. Garrard, Phys. Rev. B **16**, 2289 (1977).
[18] P. W. C. Sarvezuk, E. J. Kinast, C. V. Colin, M. A. Gusmão, J. B. M. da Cunha, and O. Isnard, J. Appl. Phys. **109**, 07E160 (2011).
[19] A. Arrott and J. E. Noakes, Phys. Rev. Lett. **19**, 786 (1967).
[20] J. Rodriguez-Carvajal, Physica B **192**, 55 (1993).
[21] L. B. McCusker, R. B. Von Dreele, D. E. Cox, D. Louer, and P. Scardi, J. Appl. Crystallogr. **32**, 36 (1999).
[22] V. F. Sears, Neutron News **3**, 26 (1992).
[23] D. T. Griffen and P. H. Ribbe, N. Jb. Miner. Abh. **137**, 54 (1979).
[24] I. Yaeger, A. H. Morrish, C. Boumford, C. P. Wong, B. M. Wanklyn, and B. J. Garrard, Solid State Commun. **28**, 651 (1978).
[25] E. F. Bertaut and P. Burlet, Solid State Commun. **5**, 279 (1967).

[26]J. E. Greedan, J. N. Reimers, C. V. Stager, and S. L. Penny, Phys. Rev. B **43**, 5682 (1991).
[27]S. Kobayashi, S. Mitsuda, M. Ishikawa, K. Miyatani, and K. Kohn, Phys. Rev. B **60**, 3331 (1999).
[28]P. Cossee and A. E. van Arkel, J. Phys. Chem. Solids **15**, 1 (1960).
[29]P. Cossee, Mol. Phys. **3**, 125 (1960).
[30]D. Gignoux and M. Schlenker, *Magnetism I: Fundamentals* (E. du Trémolet de Lacheisserie, Kluwer Academic, Dordrecht, Netherlands, 2002).
[31]D. H. Martin, *Magnetism in Solids* (Ilife Books Ltd., London, 1967).
[32]D. C. Mattis, *The Theory of Magnetism* (Harper & Row, New York, 1965).
[33]E. J. Kinast, V. Antonietti, D. Schmitt, O. Isnard, J. B. M. da Cunha, M. A. Gusmão, and C. A. dos Santos, Phys. Rev. Lett. **91**, 197208 (2003).
[34]E. G. Santos, S. R. de Oliveira Neto, E. J. Kinast, J. B. M. da Cunha, O. Isnard, and M. A. Gusmão, J. Phys. Condens. Matter **22**, 496004 (2010).